Assembly and Mechanical Properties of Phosphorus Dendrimer/Polyelectrolyte Multilayer Microcapsules

ARTICLE *in* LANGMUIR · SEPTEMBER 2005

Impact Factor: 4.46 · DOI: 10.1021/la0504208 · Source: PubMed

Assembly and Mechanical Properties of Phosphorus Dendrimer/Polyelectrolyte Multilayer Microcapsules

Byoung-Suhk Kim,[†] Olga V. Lebedeva,[†] Dong Ha Kim,[†] Anne-Marie Caminade,[‡] Jean-Pierre Majoral,[‡] Wolfgang Knoll,[†] and Olga I. Vinogradova*,[†]

Max Planck Institute for Polymer Research, Ackermannweg 10, Mainz 55128, Germany, and Laboratoire de Chimie de Coordination CNRS, 205 route de Narbonne, 31077 Toulouse Cedex 04, France

Received February 16, 2005. In Final Form: May 12, 2005

We report the preparation, characterization, and mechanical properties of polyelectrolyte/phosphorus dendrimer multilayer microcapsules. The shells of these microcapsules are composed either by alternating poly(styrenesulfonate) (PSS) and positively charged dendrimer $G_4(NH^+Et_2Cl^-)_{96}$ or by alternating poly(allylamine hydrochloride) (PAH) and negatively charged dendrimer $G_4(CH{-}COO^-Na^+)_{96}$. The same multilayers were constructed on planar support to examine their layer-by-layer growth and to measure the multilayer thickness. Surface plasmon resonance spectroscopy (SPR) showed regular linear growth of the assembly upon each bilayer deposited. We probe the mechanical properties of these polyelectrolyte/dendrimer microcapsules by measuring force−deformation curves with the atomic force microscope (AFM). The experiment suggests that they are much softer than PSS/PAH microcapsules studied before. This softening is attributed to an enhanced permeability of the polyelectrolyte/dendrimer multilayer shells as compared with multilayers formed by linear polyelectrolytes. In contrast, Young's modulus of both dendrimer-based multilayers was found to be on the same order as that of PSS/PAH multilayers.

1. Introduction

Dendrimers, monodisperse macromolecules with a regular and highly branched three-dimensional structure, have attracted attention from scientists in various fields and are important for a variety of applications.[1−5] They can be used as gene delivery agents, sensors, drug carriers, and so on. Recently, there has been significant interest in using dendrimers as building blocks for the preparation of molecularly thin films.[6] In particular, a variety of polyelectrolyte/dendrimer multilayers have been prepared. Most studies, however, were performed on supported polyelectrolyte/dendrimer multilayers, either planar[7,8] or spherical.[9] Furthermore, these previous investigations were focused on the preparation aspects of supported dendrimer based films only, and have not dealt with the mechanical properties of such multilayers.

Here we report an approach for preparing polyelectrolyte/dendrimer multilayer microcapsules by exploiting electrostatic interactions. The shell of these capsules represents a freestanding multilayer film. To date, multilayer microcapsules have been comprised of oppositely charged linear flexible polyelectrolyte,[10] polyelectrolyte/DNA,[11] polyelectrolyte/inorganic nanoparticle,[12] and polyelectrolyte/dye pairs.[13] Multilayer microcapsules containing dendrimers as building blocks represent a new system of special interest. First, such microcapsules would potentially allow two types of encapsulation: one in the dendrimers localized in the multilayer shells, and the other in the microcapsule interiors. From that point of view, such a type of microcapsule could provide a dual delivery and/or release system. Second, since the interaction of dendrimers with polyelectrolytes (and the nature of complexes formed) is most likely essentially different from those between two oppositely charged (linear) polyelectrolytes, one can expect that the physical properties (elasticity, permeability, stability) of polyelectrolyte/dendrimer microcapsules can differ dramatically from all types of microcapsules explored before. Therefore, studying these properties is not only important in the context of protection and/or release of encapsulated materials, but can also lead to a better understanding of polyelectrolytes and dendrimers in general.

To our knowledge, there have been two recent attempts to prepare polyelectrolyte/dendrimer microcapsules.[9,14] In both studies the combination of poly(styrenesulfonate) (PSS) and fourth-generation cationic poly(amidoamine) dendrimer (G_4 PAMAM) assembled on melamine formaldehyde (MF) templates was used. The PSS/G_4 PAMAM multilayers were found to be unstable toward the template removal procedure, which led to partial or complete destruction of the microcapsules. In both studies, the

* To whom correspondence should be addressed. E-mail: vinograd@mpip-mainz.mpg.de.
[†] Max Planck Institute for Polymer Research.
[‡] Laboratoire de Chimie de Coordination CNRS.

(1) Bosman, A. W.; Janssen, H. M.; Meijer, E. W. *Chem. Rev.* **1999**, *99*, 1665.
(2) Majoral, J. P.; Caminade, A. M. *Chem. Rev.* **1999**, *99*, 845−880.
(3) Caminade, A. M.; Majoral, J. P. *Acc. Chem. Res.* **2004**, *37*, 341−348.
(4) Frechet, J. M. J.; Tomalia, D. A. *Dendrimers and other dendritic polymers*; John Wiley & Sons: Chichester, UK, 2001.
(5) Newkome, G. R.; Vogtle, F.; Moorefield, C. N. *Dendrimers and dendrons*; John Wiley & Sons: Weinheim, Germany, 2001.
(6) Tsukruk, V. V. *Adv. Mater.* **1998**, *10*, 253−257.
(7) He, J. A.; Valluzzi, R.; Yang, K.; Dolukhanyan, T.; Sung, C.; Kumar, J.; Tripathy, S. K.; Samuelson, L.; Balogh, L.; Tomalia, D. A. *Chem. Mater.* **1999**, *11*, 3268−3274.
(8) Hernandez-Lopez, J. L.; Bauer, R. E.; Chang, W. S.; Glasser, G.; Grebel-Koehler, D.; Klapper, M.; Kreiter, M.; Leclaire, J.; Majoral, J. P.; Mittler, S.; Müllen, K.; Vasilev, K.; Weil, T.; Wu, J.; Zhu, T.; Knoll, W. *Mater. Sci. Eng., C* **2003**, *23*, 267−274.
(9) Khopade, A.; Caruso, F. *Nano Lett.* **2002**, *2*, 415−418.
(10) Donath, E.; Sukhorukov, G. B.; Caruso, F.; Davis, S.; Möhwald, H. *Angew. Chem.* **1998**, *37*, 2202−2205.
(11) Vinogradova, O. I.; Lebedeva, O. V.; Vasilev, K.; Gong, H.; Garcia-Turiel, J.; Kim, B. S. *Biomacromolecules* **2005**, *6*, 1495−1502.
(12) Caruso, F.; Caruso, R. A.; Mohwald, H. *Science* **1998**, *282*, 1111−1114.
(13) Dai, Z.; Voight, A.; Leporatti, S.; Donath, E.; Dähne, L.; Möhwald, H. *Adv. Mater.* **2001**, *13*, 1339.
(14) Khopade, A.; Caruso, F. *Biomacromolecules* **2002**, *3*, 1154−1162.

10.1021/la0504208 CCC: $30.25
Published on Web 06/30/2005

problem of microcapsule destruction was addressed by using smaller templates. In addition, one strategy[9] included an outer coat of PSS/poly(allylamine hydrochloride) (PAH), while the other[14] employed chemical post-modification of the shells to enhance the attractive interactions between PSS chains within the multilayer.

In the current work we assemble stable polyelectrolyte/dendrimer (both polycationic and polyanionic) microcapsules without compromising the template size and without chemical treatment, which would inevitably lead to a modification of the interactions between shell-forming polyelectrolytes and dendrimers. For a linear polyelectrolyte we use PSS and poly(allylamine hydrochloride) (PAH). Both polyelectrolytes have been intensively used before for multilayer microcapsule assembly.[10,15,16] For a cationic dendrimer, we have chosen to use positively charged *N*,*N*-disubstituted hydrazine phosphorus-containing dendrimers of the fourth generation, $G_4(NH^+Et_2Cl^-)_{96}$. Such a water-soluble and very stable cationic phosphorus dendrimer was found to present high ability as a DNA transfecting agent[17] as well as unprecedented properties as an in vivo and in vitro therapeutic agent in prion diseases.[18] In marked contrast to PAMAM, for which the interior and the surface are fully hydrophilic, all phosphorus-containing dendrimers exhibit a hydrophobic core interior and a hydrophilic charged surface.[19] Therefore, unlike PAMAM dendrimers, electrostatic interactions and complexation with PSS can take place exclusively due to surface charges. This should lead to an enhanced permeability and special mechanical properties of multilayers constituted with this class of dendrimers compared to that obtained with the same polyelectrolyte and PAMAM dendrimers. For an anionic dendrimer, we have chosen a phosphorus-containing dendrimer of the fourth generation bearing 96 carboxylate end groups, $G_4(CH-COO^-Na^+)_{96}$. This dendrimer is also water soluble and very stable, and the corresponding first generation was previously used as a building block for the elaboration of nanostructured materials.[20]

We are primarily interested in the buildup and exploitation of these ultrathin multilayer films, both supported and freestanding. Additionally, we examine the mechanical properties of assembled microcapsules. We use the atomic force microscopy (AFM) approach in combination with confocal microscopy to measure force vs deformation curves and to scan the capsule shape at different stages of compression.[16] We show that, in contrast to microcapsules with the shells formed by linear polyelectrolytes, the dendrimer-based multilayer microcapsules are highly permeable for water even in the short time scale of the AFM compression experiment. Therefore, they represent very soft composite microstructures despite the fact that Young's modulus of the shell-forming material is approximately on the same order as that for polyelectrolyte/polyelectrolyte multilayers.[21,22]

2. Experimental Section

2.1. Materials. The fluorescent dye fluorescein isothiocyanate (FITC) and shell-forming polyelectrolytes poly(sodium 4-styrenesulfonate) (PSS; $M_w \sim 70\,000$ g/mol) and poly(allylamine hydrochloride) (PAH; $M_w \sim 70\,000$ g/mol) were purchased from Sigma-Aldrich Chemie GmbH, Germany. Hydrochloric acid (HCl) and sodium chloride (NaCl) were purchased from Riedel-de Haën; Germany. All chemicals were of analytical purity or higher quality and were used without further purification.

Suspensions of monodispersed weakly cross-linked melamine formaldehyde particles (MF particles) with a radius of $r_0 = 2.0 \pm 0.1$ μm were purchased from Microparticles GmbH (Berlin, Germany).

Glass bottom dishes (0.17 mm/∅ 30 mm) with optical quality surfaces were obtained from World Precision Instruments Inc. (USA). Glass spheres (radius 20 ± 1 μm) were purchased from Duke Sci. Co., California. The glass prism and LaSFN9 substrates for surface plasmon experiments were purchased from Hellma Optik, Germany.

Water used for all experiments was purified by a commercial Milli-Q Gradient A10 system containing ion-exchange and charcoal stages, and had a resistivity of 18.2 MΩ/cm. The pH was measured by a pH meter (InoLab, Germany) with an accuracy of ±0.5.

The cationic dendrimers used in this study were the *N*,*N*-disubstituted hydrazine phosphorus-containing dendrimers of the fourth generation having 96 functional groups on the surface with cationic character, $G_4(NH^+Et_2Cl^-)_{96}$. The synthesis of $G_4(NH^+Et_2Cl^-)_{96}$ ($M_w \sim 33\,700$ g/mol) was reported in refs 17 and 23. Briefly, it was a two-step process consisting first of the reaction of 4-hydroxybenzaldehyde in basic conditions with compounds having P−Cl functions, such as $N_3P_3Cl_6$, as a core. The second step was a condensation reaction between the aldehyde and $H_2NNMeP(S)Cl_2$. Elaboration to second, third, and fourth generations was accomplished by repetition of these two steps. In each reaction cycle terminal aldehyde groups and terminal dichlorothiophosphoryl groups were introduced quantitatively and remained available for continued reactions. No protection/deprotection procedure was required, and the only byproducts were sodium chloride and water. The $P(S)Cl_2$ end groups were then modified by reaction with 2 equiv of $H_2NCH_2CH_2NEt_2$ per terminal $P(S)Cl_2$. This led to water-soluble dendrimers with positively charged ammonium surface groups. Besides ammonium groups, anionic groups such as carboxylates or alcoholates afford dendrimers soluble in water. A modified Doebner reaction of the aldehyde end groups with $CH_2(CO_2H)_2$ gives carboxylic acid end groups, whose reaction with NaOH affords the water-soluble anionic dendrimers $G_4(CH-COO^-Na^+)_{96}$ ($M_w \sim 34\,800$ g/mol).[20]

The characteristic data of both dendrimers are described in ref 17. The chemical structures of $G_4(NH^+Et_2Cl^-)_{96}$, $G_4(CH-COO^-Na^+)_{96}$, PSS, and PAH, respectively, are shown in Figure 1. According to our titration data (not shown) at least 90% of surface groups of $G_4(NH^+Et_2Cl^-)_{96}$ are charged at pH 4, and nearly all surface groups of $G_4(CH-COO^-Na^+)_{96}$ are charged at pH 10. These pH values are used below for capsule assembly.

2.2. Methods. *Capsule Preparation.* The PSS/$G_4(NH^+Et_2Cl^-)_{96}$ capsules were prepared as follows. The positively charged MF particles (50 μL of 10 wt % dispersion) as a template were incubated with 1 mL of PSS solution (1 mg/mL containing 0.5 mol/L NaCl, pH 6) for 10 min, followed by three centrifugation/rinsing cycles, and finally were dispersed in water. A 1 mL volume of a $G_4(NH^+Et_2Cl^-)_{96}$ salt-free solution (1 mg/mL, pH 4) was then added to the particle dispersion. After 30 min for adsorption, three centrifugation/wash cycles were performed (as above). These specific conditions for the dendrimer solution were chosen to fully charge the ammonium groups of the dendrimer materials. The PSS and $G_4(NH^+Et_2Cl^-)_{96}$ adsorption steps were repeated four times each to build multilayers on the MF particles. The microcapsules referred to below as $(PSS/G_4(NH^+Et_2Cl^-)_{96})_4$

(15) Lvov, Y.; Antipov, A. A.; Mamedov, A.; Möhwald, H.; Sukhorukov, G. B. *Nano Lett.* **2001**, *1*, 125−128.
(16) Vinogradova, O. I. *J. Phys.: Condens. Matter* **2004**, *16*, R1105−R1134.
(17) Loup, C.; Zanta, M. A.; Caminade, A. M.; Majoral, J. P.; Meunier, B. *Chem.−Eur. J.* **1999**, *5*, 3644−3650.
(18) Solassol, J.; Crozet, C.; Perrier, V.; Leclaire, J.; Beranger, F.; Caminade, A. M.; Meunier, B.; Dormon, D.; Majoral, J. P.; Lehmann, S. *J. Gen. Virol.* **2004**, *85*, 1791−1799.
(19) Leclaire, J.; Coppel, Y.; Caminade, A. M.; Majoral, J. P. *J. Am. Chem. Soc.* **2004**, *126*, 2304−2305.
(20) Boggiano, M. K.; Soler-Illia, G. J. A. A.; Rozes, L.; Sanchez, C.; Turrin, C. O.; Caminade, A. M.; Majoral, J. P. *Angew. Chem., Int. Ed.* **2000**, *39*, 4249.
(21) Vinogradova, O. I.; Andrienko, D.; Lulevich, V. V.; Nordschild, S.; Sukhorukov, G. B. *Macromolecules* **2004**, *37*, 1113−1117.
(22) Lulevich, V. V.; Andrienko, D.; Vinogradova, O. I. *J. Chem. Phys.* **2004**, *120*, 3822−3826.
(23) Majoral, J. P.; Caminade, A. M.; Maraval, V. *Chem. Commun.* **2002**, 2929−2942.

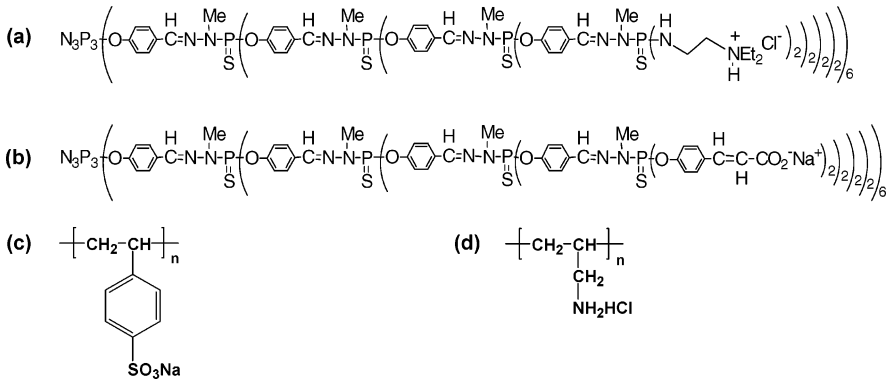

Figure 1. Structure of dendrimers ($G_4(NH^+Et_2Cl^-)_{96}$, $G_4(CH{-}COO^-Na^+)_{96}$) and polyelectrolytes (PSS, PAH) used for multilayer assembly.

capsules[24] were obtained by dissolving the MF template in HCl at pH 1.2−1.6 and washing with water three times as described before.[25] To obtain microcapsules referred to below as (PSS/$G_4(NH^+Et_2Cl^-)_{96})_5$ and (PSS/$G_4(NH^+Et_2Cl^-)_{96})_4$(PSS/PAH) microcapsules, we have deposited another, fifth, bilayer before the template dissolution. In the first case, the outer bilayer represented the same combination of PSS and $G_4(NH^+Et_2Cl^-)_{96}$. In the second case, the outer bilayer was formed by two linear polyelectrolytes, PSS and PAH. The PAH adsorption was performed by adding 1 mL of PAH solution (1 mg/mL containing 0.5 mol/L NaCl, pH 6) for 10 min, followed by the same centrifugation/wash steps as for PSS and $G_4(NH^+Et_2Cl^-)_{96}$.

The PAH/$G_4(CH{-}COO^-Na^+)_{96}$ capsules were prepared according to the same strategy. The only difference was that $G_4(CH{-}COO^-Na^+)_{96}$ dendrimer was deposited from pH 10 solutions. We also note that since the MF particles are positively charged, the first adsorbed layer was formed by $G_4(CH{-}COO^-Na^+)_{96}$ dendrimer molecules, while the last one was formed by PAH.

Microscopy. Confocal laser scanning microscopy images were taken with a commercial confocal microscope unit FV300 (Olympus, Japan) used in combination with an inverted fluorescence microscope Olympus IX70. A high-resolution (60×) bright (NA = 1.45) immersion oil objective was used. High resolution and contrast of the confocal images was achieved by the use of the fluorescent dye FITC taken at a concentration of $\sim 10^{-6}$ mol/L. The excitation wavelength was $\lambda = 488$ nm.

For scanning electron microscopy (SEM) analysis a drop of suspension of capsules was applied to a silicon wafer with sequential drying at room temperature for several hours.[26] The measurements were performed using a Gemini Leo (Zeiss) 1530 instrument operating at a working distance of 2 mm and an acceleration voltage of 0.5 kV. Since the samples were not covered with a gold layer before inspection, this low acceleration voltage was applied to avoid charging of the sample. The images were recorded using the InLens Detector.

Force Measurements. The experimental setup was described before.[22,27,28] Briefly, load (force) vs deformation curves were measured with the Molecular Force Probe device (MFP) 1D (Asylum Co., Santa Barbara, USA), which has a nanopositioning sensor. This sensor can correct piezoceramic hysteresis and creep of the AFM piezotranslator. For the force measurements we used V-shaped cantilevers (Micromash, Estonia; spring constants k = 3.0 N/m). The spring constant of the cantilever was estimated from the resonance frequency calibration plot (cantilevers catalog, Micromash, Estonia). Glass spheres were glued onto the apex of cantilevers with epoxy glue (UHU Plus, Germany). A schematic

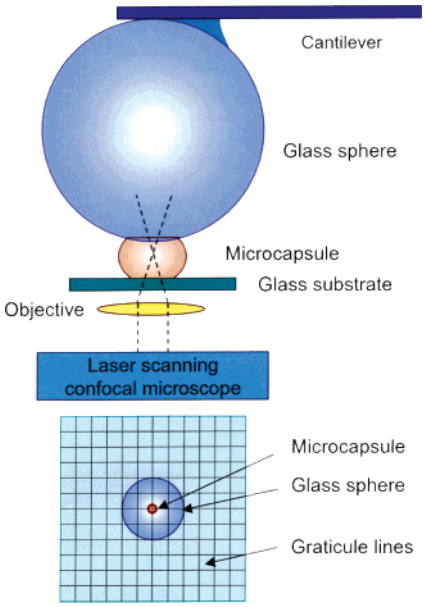

Figure 2. (top) Schematic of AFM force experiment. (bottom) Illustration of a procedure of alignment of an apex of a large glass sphere.

of the experiment is presented in Figure 2 (top). Briefly, a drop of water suspension of polyelectrolyte microcapsules was deposited onto a thin glass substrate. After a time given for capsule sedimentation, the glass sphere was centered above the apex of a chosen capsule with an accuracy of ±0.5 mm using the graticule line(s) in the optical image for alignment as shown in Figure 2 (bottom). A possible "noncoaxiality" of compression cannot affect the results of measurements since the size of a glass sphere is much larger than the size of the deformed capsule.[29] Here we performed the dynamic measurements at intervals of piezotranslator speed from 0.2 to 20 μm/s. To take confocal images of compressed capsules during force measurements, we have performed some of them in the so-called stepped regime (see ref 30 for more details). The intervals between consequent steps of the piezotranslator were 2 s. The result of the measurement represents the deflection Δ vs the position of the piezotranslator at a single approach. The load force F was determined from the cantilever deflection, $F = k\Delta$. As before, we assume that zero separation is at the point of the first measurable force.[31] Then the deformation is calculated as the difference between the position of the piezotranslator and the cantilever deflection. The diameter of the capsule was determined optically with an accuracy

(24) We remark that in our article the description of the multilayer structure will always start with the polyelectrolyte molecules. This does not reflect the consequence of layer depositions.

(25) Sukhorukov, G. B.; Donath, E.; Davis, S.; Lichtenfeld, H.; Caruso, F.; Popov, V. I.; Möhwald, H. *Polym. Adv. Technol.* **1998**, *9*, 759−767.
(26) Lulevich, V. V.; Nordschild, S.; Vinogradova, O. I. *Macromolecules* **2004**, *37*, 7736−7741.
(27) Lulevich, V. V.; Radtchenko, I. L.; Sukhorukov, G. B.; Vinogradova, O. I. *Macromolecules* **2003**, *36*, 2832−2837.
(28) Lulevich, V. V.; Vinogradova, O. I. *Langmuir* **2004**, *20*, 2874−2878.
(29) Vinogradova, O. I.; Yakubov, G. E.; Butt, H. J. *J. Chem. Phys.* **2001**, *114*, 8124−8131.
(30) Lebedeva, O. V.; Kim, B. S.; Vinogradova, O. I. *Langmuir* **2004**, *20*, 10685−10690.
(31) Lulevich, V. V.; Radtchenko, I. L.; Sukhorukov, G. B.; Vinogradova, O. I. *J. Phys. Chem. B* **2003**, *107*, 2735−2740.

of 0.2 μm and from the AFM load vs deformation curves (as in ref 31). The relative deformation ϵ of the capsule was then calculated as $\epsilon = 1 - H/(2r_0)$, where H is the minimum sphere/substrate separation.[22,31] To get reliable results, we have performed several series of force measurements. Every series included at least 10 experiments. Then the average of all force vs deformation curves was calculated.

Surface Plasmon Resonance Spectroscopy (SPR). A home-built surface plasmon resonance spectrometer was used for the thickness measurements of the multilayer films deposited on planar substrate. The sample was attached to the base of a glass prism optically matched by index oil. The beam of a He−Ne Laser (λ = 632.8 nm) with transverse magnetic polarization was reflected off the base of the prism while the prism was rotated, thus scanning the angle θ_{ex} of the incident beam relative to the sample surface. Collection of the reflected light with a photodiode (PD) mounted on a second, goniometer stage, allowed for angle-resolved reflectivity measurements (see ref 32 for more details).

To prepare substrates for SPR measurements, first a gold layer with a thickness of 50 nm was thermally evaporated on high refractive index ($n = 1.8$) LaSFN9 substrates. The gold film was then functionalized with a self-assembled monolayer of 3-mercaptopropionic acid (3MPA; Aldrich), by immersing the substrates in a 0.003 mol/L solution of 3MPA for 24 h. Such a modified surface is negatively charged in water. These substrates were used for multilayer film buildup, which was produced by assembly of four pairs of $G_4(NH^+Et_2Cl^-)_{96}$ and PSS, and an outer PSS/PAH bilayer, all deposited at conditions identical with those employed for capsule preparation. In each deposition step enough time was given to reach the adsorption equilibrium, and followed by a thorough rinsing step with Milli-Q water (for at least 20 min) to remove all excess polyelectrolyte, dendrimer, and salt. The SPR measurements were carried out in a Teflon flow cell. This allowed us to measure the thickness of the adsorbed film. The optical thickness of the samples was analyzed by "Winspall" software based on the transfer matrix evaluation method. The refractive indices of n = 1.484, 1.468, and 1.457 were used for PSS, PAH, and the dendrimer, respectively.[33−35]

3. Results and Discussion

3.1. Assembly and Stability of Polyelectrolyte/Dendrimer Microcapsules. Exposing $(PSS/G_4(NH^+Et_2Cl^-)_{96})_4$ coated MF particles to pH 1.1−1.6 HCl solution results in the dissolution of the templates. The dissolved MF is expelled from the core via permeation through the multilayers upon dissolution and washing.[10,36] Evidence of capsule formation was directly obtained from confocal scanning microscopy (Figure 3a). The capsules were, however, found to be fragile and often broken. The percentage of unbroken capsules was quite low (<20%). It is likely that the microcapsule shells are destroyed during their stretching,[37] which accompanies the MF dissolutions[36] (and probably also during the multiple centrifugation/washing steps). Indeed, in the case of polyelectrolyte/dendrimer multilayers the linear polyelectrolytes could align under inner osmotic pressure, but definitely not the dendrimers. Since the energy of stretching of the multilayer shell is proportional to its thickness, h,[16,22] we have deposited one additional bilayer of PSS/$G_4(NH^+Et_2Cl^-)_{96}$ to increase the rupture strength of the multilayer. However, this strategy led to practically the same amount of broken capsules. We, therefore, decided to cover four PSS/$G_4(NH^+Et_2Cl^-)_{96}$ bilayers by a stabilizing coating of a standard PSS/PAH pair similarly to ref 9. This step, indeed, increased the stability of dendrimer-containing capsules. The absolute majority of them (>80%) has ideal spherical shape (Figure 3b).

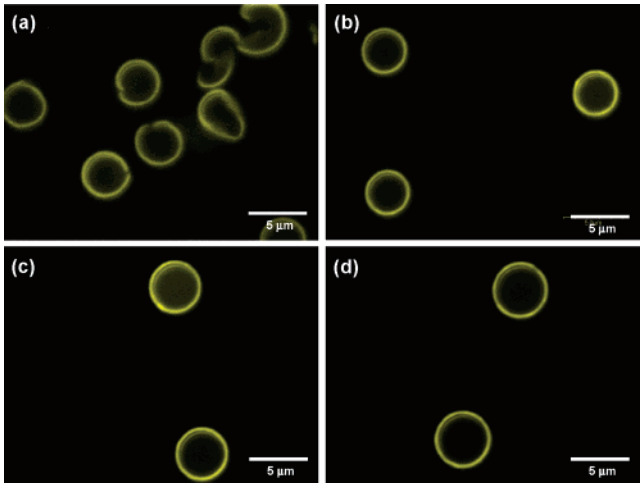

Figure 3. Confocal images of polyelectrolyte/dendrimer microcapsules. The multilayer shell is composed of $(PSS/G_4(NH^+Et_2Cl^-)_{96})_4$ (a), $(PSS/G_4(NH^+Et_2Cl^-)_{96})_4$(PSS/PAH) (b), $(PAH/G_4(CH-COO^-Na^+)_{96})_4$ (c), and $(PAH/G_4(CH-COO^-Na^+)_{96})_4$-(PSS/PAH) (d).

Exposing $(PAH/G_4(CH-COO^-Na^+)_{96})_4$ coated MF particles to the same HCl solution leads to a formation of a suspension of unbroken microcapsules (Figure 3c). This result represents the first successful attempt to prepare dendrimer-based capsules without a protective polyelectrolyte bilayer coating. To the best of our knowledge, such an assembly was never reported before. The same remark concerns the use of anionic dendrimers as building blocks for multilayer microcapsule formation. To evaluate the role of protective PSS/PAH coating in determining the stiffness of microcapsules and to compare anionic and cationic dendrimer based multilayer shells, we have also prepared five bilayer $(PAH/G_4(CH-COO^-Na^+)_{96})_4$(PSS/PAH) microcapsules (Figure 3d).

Thus, we have not managed to assemble capsules without a protective PSS/PAH bilayer by using a strong polyelectrolyte PSS alternating with the charged dendrimer, but we have succeeded in this by using a weak polyelectrolyte, PAH. This apparently unexpected result might be connected to the fact that in the case of $(PSS/G_4(NH^+Et_2Cl^-)_{96})_4$ capsules the outer layer is formed by dendrimers, while in the case of $(PAH/G_4(CH-COO^-Na^+)_{96})_4$ capsules it is formed by polyelectrolytes. One can speculate that the possibility for an outer PAH to align under inner osmotic pressure allows increasing the rupture strength of the shells.

The outer polymer layer/bilayer not only increases the rupture strength of dendrimer-based microcapsules, but also changes their surface morphology. We have taken and analyzed SEM images of microcapsules with an outer layer formed by a dendrimer, with an outer layer formed by a polyelectrolyte, and with the polyelectrolyte bilayer coating, respectively. In the first case the microcapsules contained many more folds with sharper edges as compared with previous observations,[26] which already indicates an enhanced fragility. In the second case, the surface morphology looked a bit smoother. In the case of a protective PSS/PAH coating, it was similar to what was observed before for PSS/PAH microcapsules[26] (Figure 4). One can, therefore, suggest that the outer polyelectrolyte

(32) Knoll, W. *Annu. Rev. Phys. Chem.* **1998**, *49*, 569−638.
(33) Ruths, J.; Essler, F.; Decher, G.; Riegler, H. *Langmuir* **2000**, *16*, 8871.
(34) Vasilev, K.; Knoll, W.; Kreiter, M. *J. Chem. Phys.* **2004**, *120*, 3439−3445.
(35) Picart, C.; Sengupta, K.; Schilling, J.; Maurstad, G.; Ladam, G.; Bausch, A. R.; Sackmann, E. *J. Phys. Chem. B* **2004**, *108*, 7196−7205.
(36) Gao, C. Y.; Moya, S.; Lichtenfeld, H.; Casoli, A.; Fiedler, H.; Donath, E.; Mohwald, H. *Macromol. Mater. Eng.* **2001**, *286*, 355−361.
(37) Kim, B. S.; Vinogradova, O. I. *J. Phys. Chem. B* **2004**, *108*, 8161−8165.

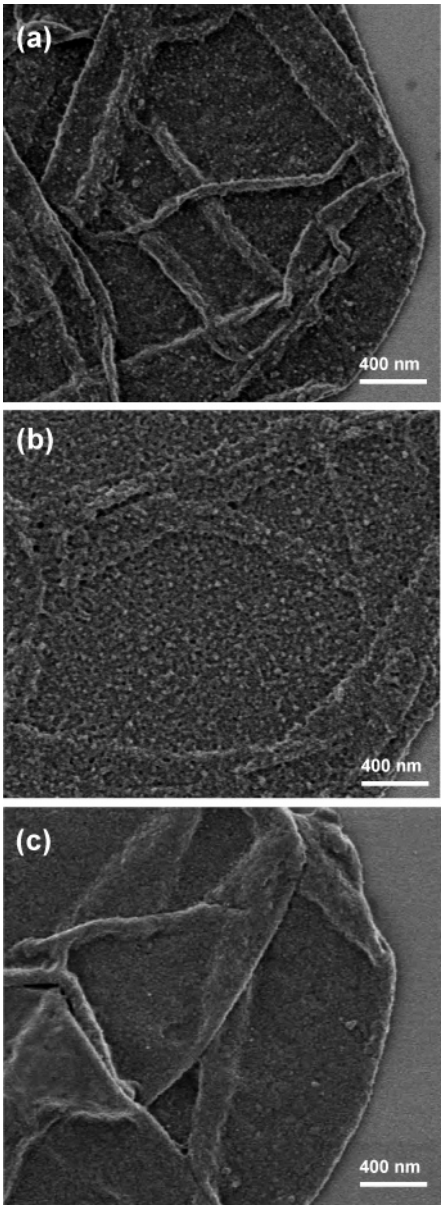

Figure 4. SEM images of dried $(PSS/G_4(NH^+Et_2Cl^-)_{96})_4$ (a), $(PAH/G_4(CH-COO^-Na^+)_{96})_4$ (b), and $(PSS/G_4(NH^+Et_2Cl^-)_{96})_4$-(PSS/PAH) (c) microcapsules.

layer and especially the bilayer lead to a self-healing of the multilayer. In other words, it allows buildup of smoother shells.

3.2. Characterization of the Multilayers. Similar dendrimer/polyelectrolyte multilayers were constructed on a planar support to characterize their layer-by-layer growth. Figure 5 illustrates the kinetics of this process for $(G_4(NH^+Et_2Cl^-)_{96}/PSS)_4(PAH/PSS)$ multilayers. The thick, thin, and dashed curves indicate the adsorption/desorption steps for $G_4(NH^+Et_2Cl^-)_{96}$, PSS, and PAH, respectively. It is seen that the addition of each layer leads to an increase in the reflectivity. The analysis of the plateau regions of the kinetic curves confirms that the adsorption time used during the assembly of microcapsules allows reaching equilibrium. The washing of the samples leads to a decrease in intensity, small in the case of $G_4(NH^+Et_2Cl^-)_{96}$ and rather significant for PSS or PAH. The almost instantaneous increase in the reflectivity signal after injection of the (linear) polyelectrolyte (PAH and PSS) solutions, and its rather rapid decrease upon rinsing the sample cell with pure water, could originate

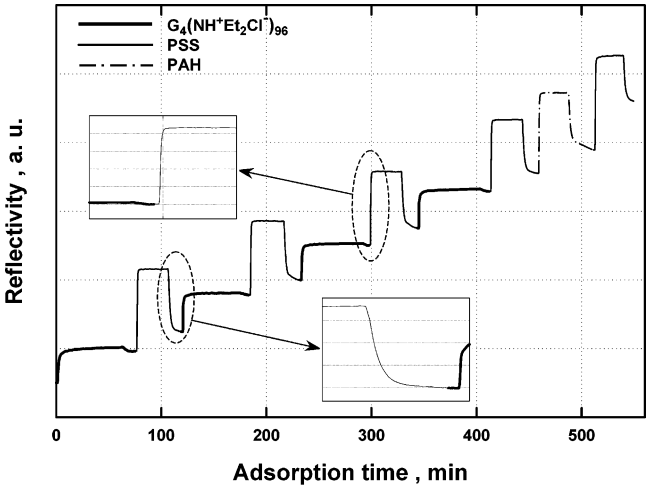

Figure 5. Kinetic SPR scan profile of consecutive deposition of four bilayers of $PSS/G_4(NH^+Et_2Cl^-)_{96}$ followed by PAH/PSS bilayer on 3MPA coated Au substrate. The thick and thin solid curves indicate the adsorption steps of $G_4(NH^+Et_2Cl^-)_{96}$ and PSS layers, respectively. The dashed curve represents the adsorption of PAH layer.

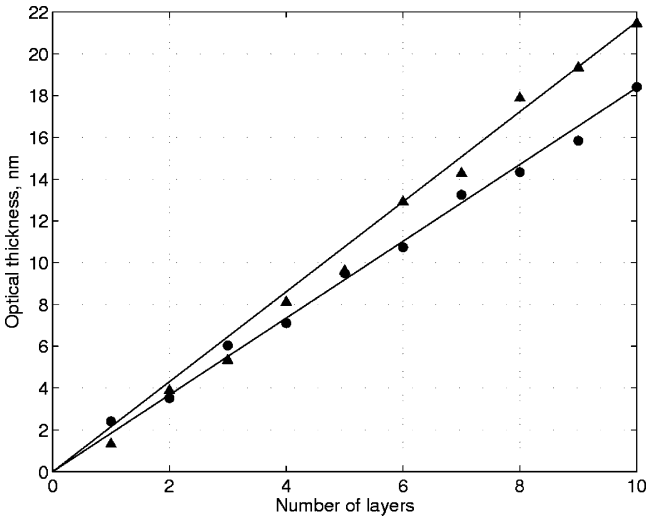

Figure 6. Thickness of $(PSS/G_4(NH^+Et_2Cl^-)_{96})_4(PSS/PAH)$ and $(PAH/G_4(CH-COO^-Na^+)_{96})_4(PSS/PAH)$ films as a function of deposited layers. (●) Odd layers are from $G_4(NH^+Et_2Cl^-)_{96}$ (1−7) and PAH (9). Even layers are from PSS. (▲) Odd layers are from PAH. Even layers are from $G_4(CH-COO^-Na^+)_{96}$ (2−8) and PSS (10).

from either a refractive index change (of the polymer solution versus the pure buffer) or a rapid adsorption/desorption of polyelectrolyte to/from the interface. Since all polyelectrolyte solutions were only 1 mg/mL in concentration, the former explanation can be ruled out. The reflectivity change, hence, reflects a substantial adsorption of linear polymer upon the injection of the solution beyond a mere monolayer, which, however, is again rapidly desorbing upon rinsing the sample with pure water. This behavior is in remarkable contrast to the adsorption behavior of the dendrimers (and confirms that a mere index change can be ruled out since the dendrimer concentrations were the same as those of the linear polyelectrolyte solutions). Similar features were observed for $(PAH/G_4(CH-COO^-Na^+)_{96})$ multilayers (not shown).

Figure 6 shows the equilibrium optical thickness of the dendrimer-based films as a function of the number of deposition cycles which was obtained by converting the accumulated shift of resonance angles in scan mode SPR

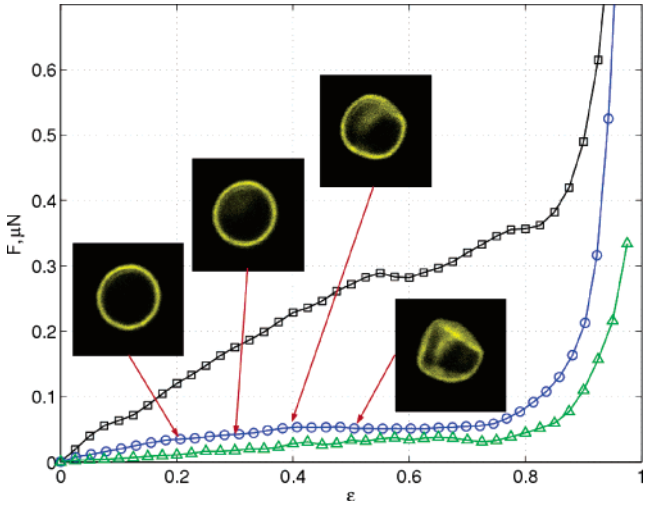

Figure 7. Average force−deformation curve measured for $(PSS/G_4(NH^+Et_2Cl^-)_{96})_4(PSS/PAH)$ microcapsules (blue circles) and $(PAH/G_4(CH{-}COO^-Na^+)_{96})_4(PSS/PAH)$ (green triangles). For comparison, the typical deformation profile obtained for $(PSS/PAH)_5$ microcapsules is also included (black squares). For all curves only every 15th point is shown. Insets show confocal images (equatorial cross section) of deformed dendrimer/polyelectrolyte capsules at given relative deformation, ϵ.

spectroscopy (not shown here). The experiment shows the regular linear growth of the film, which is consistent with multilayer ordering. In the case of a $PSS/G_4(NH^+Et_2Cl^-)_{96}$ film, the bilayer thickness is found to be ∼3.6 nm. Here, the thickness of a dendrimer monolayer is ∼2.4 nm and that of a PSS monolayer is ∼1.2 nm. Since the $G_4(NH^+Et_2Cl^-)_{96}$ dendrimer in solution has a diameter of 5−7 nm,[19] the measured thickness of a dendrimer monolayer indicates spreading of dendritic molecules, which become highly flattened during adsorption and complexation. The strong electrostatic interactions of the ionic groups of charged dendrimers and polyelectrolytes are likely responsible for these spreading and flattening reorganizations. Similar effects were observed before for different types of dendrimers.[6,9,38,39] In the case of a $PAH/G_4(CH{-}COO^-Na^+)_{96}$ film, the bilayer thickness is found to be ∼4.5 nm. The thickness of dendrimer and PAH monolayer was ∼3.1 nm and ∼1.4 nm, respectively. A larger thickness of an anionic dendrimer monolayer might be attributed to weaker electrostatic interactions of the ionic groups of charged dendrimers and polyelectrolytes.

3.3. Deformation Profiles. Figure 7 shows the average force vs deformation profiles for $(PSS/G_4(NH^+Et_2Cl^-)_{96})_4$-(PSS/PAH) and $(PAH/G_4(CH{-}COO^-Na^+)_{96})_4(PSS/PAH)$ microcapsules. For comparison, the force curve obtained before for $(PSS/PAH)_5$ microcapsules is included. One can see that, compared to the linear polyelectrolyte microcapsules, the $(PSS/G_4(NH^+Et_2Cl^-)_{96})_4(PSS/PAH)$ and $(PAH/G_4(CH{-}COO^-Na^+)_{96})_4(PSS/PAH)$ capsules are much softer. The capsules containing PAH and anionic dendrimers are softer than capsules containing PSS and cationic dendrimers. The force vs deformation profiles contain an extended regime of deformation at quasi-constant load. As we have shown before,[9,26,27,31] such a plateau normally indicates a very rapid drainage of the inner solution. This is confirmed by a confocal scan, which shows that the equatorial cross section of the capsule shells deviates from a circular shape already at $\epsilon \geq 0.2$. For PSS/PAH microcapsules this shape was normally circular up to $\epsilon = 0.35-0.45$ or even larger values.[22,26] We have also measured the force vs deformation curves for $(PAH/G_4(CH{-}COO^-Na^+)_{96})_4$ microcapsules (not shown). These capsules were found to be the softest. Moreover, a regular force profile was observed only up to $\epsilon = 0.15-0.2$. At larger deformations, $(PAH/G_4(CH{-}COO^-Na^+)_{96})_4$ microcapsules have given irregularities (oscillations) in the force curves, which is most likely related to the local ruptures of the shells. Thus, these capsules seem to be highly fragile, indicating that a single polyelectrolyte layer is probably not enough to provide a resistance to stretching (expected even for highly permeable capsules at large ϵ since their free area is getting smaller with deformation).

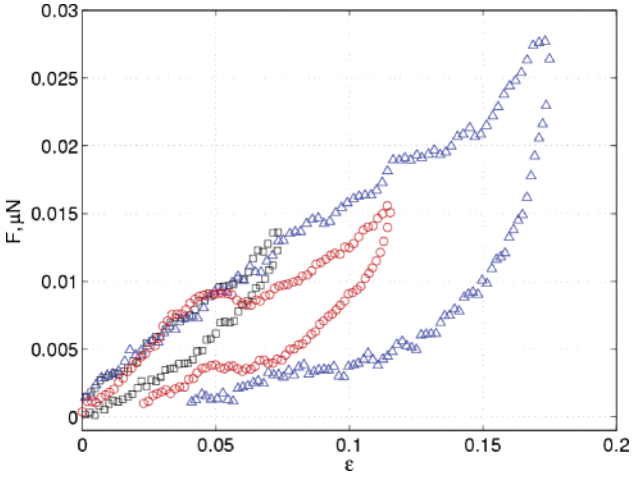

Figure 8. Typical loading/unloading cycles for dendrimer-based capsules at small deformations. Only every second point is shown.

To examine this drainage/permeability issue more closely, we have studied the reversibility of deformations. Figure 8 includes typical loading/unloading cycles at small deformations for all capsules studied here. It is seen that the deformation can be treated as being completely reversible only for $\epsilon \leq 0.05$ (cf. $\epsilon \leq 0.2-0.25$ for PSS/PAH capsules[22,28]). Already at $\epsilon = 0.1-0.15$ the deformation is becoming only partially reversible. Here we also observe a large hysteresis. We note that we have not detected an influence of the driving speed in the interval used, as we observed before for a situation of finite permeability of the shells.[22,28,31] It is likely that the (drainage) permeability is so high that the changes in the driving speed within the interval used do not make any contribution to the force.

Thus, the $PSS/G_4(NH^+Et_2Cl^-)_{96}$ and $PAH/G_4(CH{-}COO^-Na^+)_{96}$ microcapsules are very soft compared with PSS/PAH microcapsules, and one reason for this is connected to the enhanced permeability, allowing the inner solution to drain out easily even in the short time of the AFM force experiment. We have explored whether this enhanced permeability correlates with a difference in the elastic properties of the multilayers. In fact, softer multilayer films might be expected in the case of weaker ionic cross-links, different organization of compounds in the multilayers, and different conformation changes.

If the shell is infinitely permeable to water, and provided that relative deformations are small, the measured force should be entirely due to the bending of the multilayer shell near the contact line. In this case as a rough estimate one can use[16,28]

$$F \sim \frac{\pi E h^2 \sqrt{\epsilon}}{2\sqrt{2}} \quad (1)$$

(38) Tsukruk, V. V.; Rinderspracher, R.; Bliznyik, V. N. *Langmuir* **1997**, *13*, 2171.
(39) Sheiko, S. S.; Musafarov, A. M.; Winkler, R. G.; Getmanova, E. V.; Echert, G.; Reineker, P. *Langmuir* **1997**, *13*, 4172.

where E is Young's modulus. According to our SPR measurements the thickness, h, of $(PSS/G_4(NH^+Et_2Cl^-)_{96})_4(PSS/PAH)$ shell is equal to 18.4 nm, and that of $(PAH/G_4(CH-COO^-Na^+)_{96})_4(PSS/PAH)$ is equal to 21.45 nm. The data at $\epsilon \leq 0.1$ are well fitted for the first multilayer with $E = 150$ MPa and for the second with $E = 80$ MPa (Figure 9). This Young's modulus is smaller than that (~200 MPa) found for PSS/PAH multilayers before,[16,21] but remains in the same order of magnitude. Although we do not and still cannot claim universality, this result might indicate that the stiffness of building blocks for multilayer formation is much less important compared with the number and strength of ionic cross-links. Clearly, more work is needed to confirm this hypothesis, although a similar conclusion might be drawn from our recent DNA/PAH capsule study.[11] The twice smaller Young's modulus found in the case of PAH used as a polyelectrolyte in the multilayer assembly is consistent with this idea. Indeed, PAH is a much weaker polyelectrolyte than PSS, so the number of ionic cross-links with the oppositely charged dendrimer should be smaller.[40] We also fitted the initial part of a force profile measured for $(PAH/G_4(CH-COO^-Na^+)_{96})_4$ capsules, by using the value of $h = 17.88$ nm. The value of Young's modulus obtained, $E = 80$ MPa, coincides with that obtained for the same capsules, but coated by a PSS/PAH bilayer. This allows the suggestion that one bilayer coating does not introduce discernible changes in Young's modulus values.

An alternative model, which neglects water drainage through the shells[22]

$$F \sim 4\pi E h r_0 \epsilon^3 + \frac{\pi E h^2 \sqrt{\epsilon}}{2\sqrt{2}} \qquad (2)$$

was previously used to describe the deformation of capsules made from linear polyelectrolytes.[16,22] Theoretical curves calculated using Young's modulus, $E = 150$ and 80 MPa, found for all three types of capsules and $h = 18.4$, 21.45, and 17.88 nm are included in Figure 9. It is quite evident then that this model is not suitable for a description of the compression of polyelectrolyte/dendrimer capsules studied here. Therefore, the major difference for the capsules made from linear polyelectrolytes concerns the drainage issue.

(40) Lebedeva, O. V.; Kim, B. S.; Vasilev, K.; Vinogradova, O. I. *J. Colloid Interface Sci.* **2005**, *284*, 455–462.

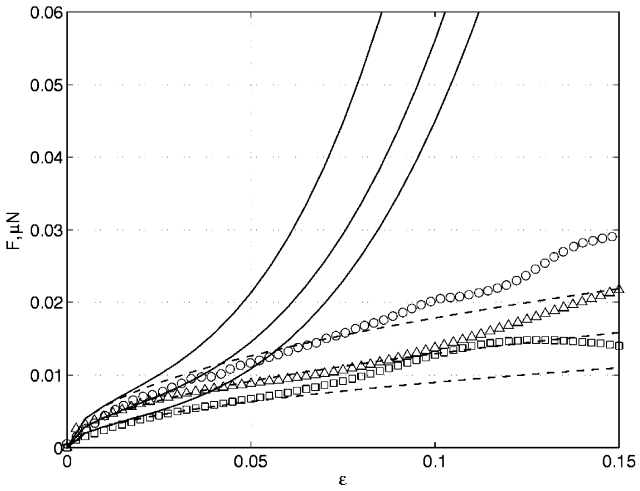

Figure 9. Average force–deformation curves at small relative deformations measured for $(PSS/G_4(NH^+Et_2Cl^-)_{96})_4(PSS/PAH)$ (circles), $(PAH/G_4(CH-COO^-Na^+)_{96})_4(PSS/PAH)$ (triangles), and $(PAH/G_4(CH-COO^-Na^+)_{96})_4$ (squares) microcapsules. Only every second point is shown. Fit to eq 1 gives $E = 150$, 80, and 80 MPa, respectively (dashed curves from top to bottom). Solid curve (from left to right) shows the force vs relative deformation profile expected for impermeable capsules (eq 2) with the same Young's modulus.

4. Conclusions

We have shown that $(PSS/G_4(NH^+Et_2Cl^-)_{96})_4$ and $(PAH/G_4(CH-COO^-Na^+)_{96})_4$ microcapsules can be obtained by dissolution of multilayer-coated colloidal templates. The microcapsules prepared present novel dual delivery/release systems that are potentially useful for a range of applications. Our experiment has also demonstrated that these capsules are much softer than (linear) polyelectrolyte/polyelectrolyte (PSS/PAH) microcapsules studied before. This softening was shown to be mostly due to a rapid drainage of water from the compressed microcapsules. The Young's modulus of the $G_4(NH^+Et_2Cl^-)_{96}$ and $PAH/G_4(CH-COO^-Na^+)_{96}$ based shell materials is also found to be smaller than that for PSS/PAH multilayers.

Acknowledgment. We thank G.Glasser for taking SEM images and V.Ball for helpful discussions. Partial support for this work from the Alexander von Humboldt Foundation (B.-S.K.) and the Deutsche Forschungsgemeinschaft (MU 334/22-2 and SFB 625) is gratefully acknowledged.

LA0504208